

## ARTICLE

# Structural and functional characterization of the cytotoxic protein ledodin, an atypical ribosome-inactivating protein from shiitake mushroom (*Lentinula edodes*)

Lucía Citores<sup>1</sup> | Sara Ragucci<sup>2</sup> | Rosita Russo<sup>2</sup> | Claudia C. Gay<sup>3</sup> |  
 Angela Chambery<sup>2</sup> | Antimo Di Maro<sup>2</sup>  | Rosario Iglesias<sup>1</sup> | José M. Ferreras<sup>1</sup> 

<sup>1</sup>Department of Biochemistry and Molecular Biology and Physiology, Faculty of Sciences, University of Valladolid, E-47011 Valladolid, Spain

<sup>2</sup>Department of Environmental, Biological and Pharmaceutical Sciences and Technologies (DiSTABiF), University of Campania 'Luigi Vanvitelli', Via Vivaldi 43, 81100 Caserta, Italy

<sup>3</sup>Laboratory of Protein Research, Institute of Basic and Applied Chemistry of Northeast Argentina (UNNE-CONICET), Faculty of Exact and Natural Sciences and Surveying (UNNE), Corrientes, Argentina

## Correspondence

Rosario Iglesias and José M. Ferreras, Department of Biochemistry and Molecular Biology and Physiology, Faculty of Sciences, University of Valladolid, E-47011 Valladolid, Spain. Email: [riglesias@uva.es](mailto:riglesias@uva.es) and [josemiguel.ferreras@uva.es](mailto:josemiguel.ferreras@uva.es)

## Funding information

Consejería de Educación, Junta de Castilla y León, Grant/Award Number: VA033G19; Junta de Castilla y León, Grant/Award Numbers: BIO/VA17/15, BIO39/VA39/14

**Review Editor:** Aitziber L. Cortajarena

## Abstract

We have purified ledodin, a cytotoxic 22-kDa protein from shiitake mushroom (*Lentinula edodes*) consisting of a 197 amino acid chain. Ledodin possessed N-glycosylase activity on the sarcin-ricin loop of mammalian 28S rRNA and inhibited protein synthesis. However, it was not active against insect, fungal, and bacterial ribosomes. In vitro and in silico studies suggested that ledodin exhibits a catalytic mechanism like that of DNA glycosylases and plant ribosome-inactivating proteins. Moreover, the sequence and structure of ledodin was not related to any protein of known function, although ledodin-homologous sequences were found in the genome of several species of fungi, some edible, belonging to different orders of the class Agaricomycetes. Therefore, ledodin could be the first of a new family of enzymes widely distributed among this class of basidiomycetes. The interest of these proteins lies both, in the fact that they can be a toxic agent of some edible mushrooms and in their application in medicine and biotechnology.

## KEYWORDS

protein synthesis (inhibition), ribosome-inactivating protein (RIP), ribotoxin, rRNA N-glycosylase, shiitake (*Lentinula edodes*), toxin

Lucía Citores and Sara Ragucci contributed equally to this work.

This is an open access article under the terms of the [Creative Commons Attribution-NonCommercial-NoDerivs](https://creativecommons.org/licenses/by-nc-nd/4.0/) License, which permits use and distribution in any medium, provided the original work is properly cited, the use is non-commercial and no modifications or adaptations are made.

© 2023 The Authors. *Protein Science* published by Wiley Periodicals LLC on behalf of The Protein Society.

## 1 | INTRODUCTION

Shiitake (*Lentinula edodes* [Berk.] Pegler) is the second most consumed mushroom worldwide, after the button, and its consumption is continuously increasing (Chung et al., 2022); China alone produced more than 11 million tons in 2019 accounting for about 30% of this country's mushroom production (Sharma et al., 2022). Shiitake has been reported to have great nutritional value and that its consumption provides many benefits due to its fiber content, nutrients, and wide range of functional metabolites (Niego et al., 2021). Because the extracts and pure compounds of shiitake have shown antibacterial, antifungal, cytostatic, antioxidant, anticancer, and immunomodulatory activities, different shiitake-derived products are on the market and sold as dietary supplements (Niego et al., 2021). Some of these compounds such as the polysaccharide lentinan (Sheng et al., 2021), the protein lentin (Ngai & Ng, 2003), or the alkaloid eritadenine (Afrin et al., 2016) have shown anticarcinogenic, antiviral, and antihypertensive activities, respectively. However, the consumption of shiitake also presents risks, especially when raw or undercooked mushrooms are consumed, being the most common clinical presentations linear flagellated dermatitis, pruritus, fever, diarrhea, and mucosal ulcers, attributed to the lentinan polysaccharide (Nguyen et al., 2017).

The study of the cytotoxic properties of proteins and other molecules of fungi has always aroused great interest, on the one hand, to know and avoid the harmful effects of mushroom consumption, and on the other because they have important biotechnological applications (Fang & Ng, 2011; Niego et al., 2021). Some cytotoxic proteins are powerful inhibitors of protein synthesis. Among the most studied and most useful are plant ribosome inactivating proteins (RIPs; Citores et al., 2013; Di Maro et al., 2014) and fungal ribotoxins (Olombrada et al., 2017).

RIPs from plants are rRNA N-glycosylases (EC 3.2.2.22) that catalyze the elimination of a specific adenine located in the sarcin-ricin loop (SRL) of 28S ribosomal RNA from animals (Citores et al., 2013; Di Maro et al., 2014). The elimination of this adenine inactivates the ribosomes, which leads to the irreversible inhibition of protein synthesis and therefore cell death (Citores et al., 2013; Di Maro et al., 2014). RIPs have been classified according to their structure into type 1 RIPs (a polypeptide chain with N-glycosylase activity) and type 2 RIPs (an A chain with enzymatic activity and a B chain with lectin activity, linked by a disulfide bond; Di Maro et al., 2014). Most RIPs have been isolated and characterized from angiosperm plants, including edible species,

while one has been obtained from algae and a few from bacteria or fungi (Di Maro et al., 2014; Landi, Hussain, et al., 2022). Although the structure, activity, and mode of action of RIPs are known, their biological function is unclear. It has been proposed that these proteins could play an important role in the defense of plants against viruses, fungi, and insects (Citores et al., 2021; Zhu et al., 2018).

Fungal ribotoxins are highly specific rRNA ribonucleases (EC 4.6.1.23) that catalyze the cleavage of a phosphodiester bond on the SRL of 28S rRNA (Olombrada et al., 2017). Only five ribotoxins produced by four species of ascomycetes have been isolated (Olombrada et al., 2017). Recently, cytotoxic ribonucleases have been found in the edible fruiting bodies of some basidiomycetes. These proteins were initially called ribotoxins and later ribotoxin-like proteins (RL-Ps), since, although they show the same enzymatic activity, they exhibit a different sequence and structure (Landi, Hussain, et al., 2022). It has been postulated that ribotoxins and RL-Ps could have an insecticidal (Olombrada et al., 2017) and fungicidal role (Citores et al., 2018; Citores et al., 2019).

Due to the translation-inhibiting and apoptotic activities of RIPs and ribotoxins, they have been used in medicine mainly as the toxic part of immunotoxins, that is, toxins linked to an antibody specifically directed against a target, usually an antigen from a tumor cell (Citores et al., 2013; Olombrada et al., 2017). RIPs have also been used in agriculture to increase crop resistance to viruses, insects, and fungi by designing transgenic plants (Citores et al., 2021; Zhu et al., 2018).

Investigating the cytotoxic effects of fungal proteins, we have found a new type of toxin in shiitake that we have named ledodin. Ledodin has been shown to be a cytotoxic protein that strongly inhibits protein synthesis and displays N-glycosylase activity on the SRL of 28S rRNA from mammals. The sequence and structure of ledodin are not related to any protein of known function and although its biological role is unknown, its activities point to an antifeedant role. A preliminary database search has allowed us to find that other fungi contain homologous proteins in their genome, therefore, ledodin could be the first of a family of toxins present in a considerable number of fungi, some of them edible. The discovery of a new family of cytotoxic proteins in mushrooms is of great health interest, both for their involvement in food safety and for their potential applications in biomedicine and biotechnology, since proteins with the same cellular target are used for the construction of immunotoxins, conjugates, engineered proteins, or nanocapsules for the experimental therapy of cancer or viral diseases (Citores et al., 2013; Citores et al., 2021).

## 2 | RESULTS AND DISCUSSION

### 2.1 | Isolation of ledodin

The study of cytotoxic proteins in mushrooms such as shiitake raises great interest both for its involvement in food safety and for being an excellent source of proteins with applications in biotechnology (Niego et al., 2021). Since many toxins are translation inhibitors, we employed a method used for the purification of RIPs from plants (Barbieri et al., 1987; Iglesias et al., 2022), with the aim of finding and purifying inhibitors of protein synthesis. A crude extract was prepared from 100 g of shiitake fresh fruiting bodies. Then, an acidified crude extract was obtained and subjected to ion exchange chromatography in a column of SP-Sepharose. Once the sample was loaded, the column was washed with sodium acetate and sodium phosphate, and finally eluted with NaCl. The protein eluted with NaCl was dialyzed and subjected to chromatography through SP-Sepharose with a linear gradient of NaCl (Figure 1a). The fractions obtained in the chromatography were analyzed by SDS-PAGE under reducing conditions and tested in a cell-free protein synthesis system. From 40 to 50 mM of NaCl eluted a protein that we named ledodin (Figure 1a, shaded area); and from 25 to 35 mM of NaCl another protein (Figure 1a, peak #1) with the same molecular weight, amino terminal sequence and enzymatic properties (Figure 1b–d) than ledodin. Although the latter protein could be ledodin with some modification, to be sure that we were working with a pure protein, subsequent studies were carried out only with ledodin. The yield of the current preparation was 2.7 mg of ledodin per 100 g of fresh starting tissue (equivalent to 13.4 mg per 100 grams of dry weight). SDS-PAGE analysis in the presence of 2-mercaptoethanol showed that ledodin consists of a single polypeptide chain with a molecular weight of 22 kDa (Figure 1b). As shown in Figure 1c, ledodin is not glycosylated, as it was not stained with the glycoprotein staining that did dye quinoine, a type 1 RIP obtained from quinoa seeds (Ragucci et al., 2021). Interestingly, ledodin was shown to be a potent inhibitor of protein synthesis in the rabbit reticulocyte lysate system (Figure 1d), with an  $IC_{50}$  (concentration inhibiting 50% of protein synthesis) of 19 ng/mL (0.86 nM). As indicated above, the protein eluting at peak #1 showed the same  $IC_{50}$  value. This  $IC_{50}$  is 30-fold higher than that shown by BE27 (Figure 1d), a very active type 1 RIP obtained from beet leaves (Iglesias et al., 2015), but it is within the range of those already published, for both, plant RIPs (between 0.03 and 4 nM; Barbieri et al., 1993; Citores et al., 2013) and fungal RIPs (between 0.5 and 17 nM; Landi, Hussain, et al., 2022).

### 2.2 | Enzymatic activity of ledodin

Among the most studied plant and fungal enzymes that inhibit protein synthesis are ribonucleases (RNases), ribotoxins, ribotoxin-like proteins (RL-Ps), and RIPs. RNases encompass several superfamilies of enzymes that can inhibit protein synthesis by degrading the different types of RNA involved in this process (Saxena et al., 1991). RNases are very abundant in fungi and many of them have very interesting medicinal properties (Fang & Ng, 2011). Five ribonucleases have been described in shiitake, three of which are found in the fruiting bodies (Kobayashi, Hara, et al., 2000; Kobayashi, Kumagai, et al., 2000). Ribotoxins (such as  $\alpha$ -sarcin, restrictocin and mitogillin), RL-Ps (such as ageritin) and RIPs (such as ricin, PAP and BE27), are much more specific enzymes whose target is the SRL of the 28S ribosomal RNA of animal cells (Citores et al., 2013; Di Maro et al., 2014; Landi, Hussain, et al., 2022; Olombrada et al., 2017). This loop is conserved in all organisms and is involved in the interaction of elongation factors with the ribosome (Citores et al., 2013; Di Maro et al., 2014; Olombrada et al., 2017). Ribotoxins and RL-Ps are highly specific rRNA endoribonucleases, present in fungi, that catalyze the cleavage of the phosphodiester bond between guanosine 4325 and adenosine 4326 in the 28S rRNA from rat (or the equivalent phosphodiester bond in ribosomes from other organisms), releasing a fragment of about 460 nucleotides (in the case of rat ribosomes) at the 3' end of 28S rRNA, that is diagnostic of the catalytic action of ribotoxins and RL-Ps (Endo & Wool, 1982; Landi, Hussain, et al., 2022). RIPs are a group of proteins with rRNA N-glycosylase activity present in a large number of plants that catalyze the removal of adenine 4324 from the 28S rRNA of rat (or the adenine equivalent in ribosomes from other organisms) which makes the phosphodiester bond between G4323 and A4324 susceptible to rupture with acid aniline, thus releasing the same diagnostic fragment (Endo et al., 1987).

To determine what kind of inhibitor ledodin is, we carried out several enzymatic assays. First, we found that ledodin had no ribonuclease activity, since 8  $\mu$ g/mL had no effect on yeast RNA, whereas the effect of pancreatic RNase A was evident at 10,000-fold lower concentration (Figure S1). To investigate whether ledodin had endonuclease activity or N-glycosylase activity on the SRL of ribosomal RNA, we carried out the Endo's assay on ribosomes from two animals, from rabbit and from the mealworm insect. As shown in Figure 1e, in the absence of aniline no fragment was produced when rabbit reticulocyte lysate was incubated with ledodin, but in the presence of aniline a fragment of 460 nucleotides identical to that produced by the RIP BE27 was released. This clearly

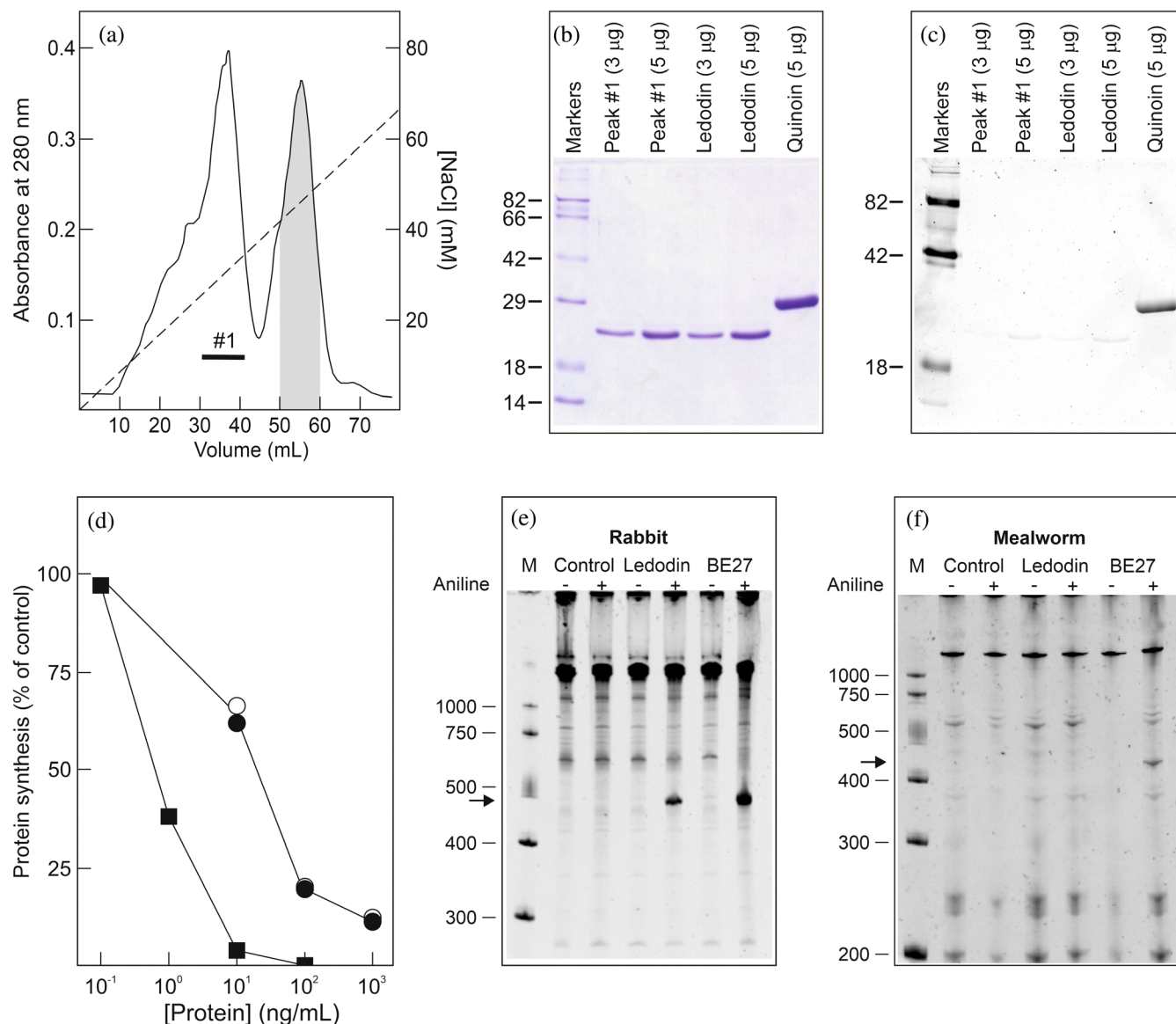


**FIGURE 1** Purification of ledodin from the protein fraction eluted with NaCl in SP-Sepharose. (a) Chromatography in SP-Sepharose FF was performed with a NaCl gradient as indicated in Section 4. The  $A_{280}$  is represented by a solid line and the NaCl concentration by a dashed line. The shaded fraction contained ledodin, the fraction marked with the horizontal line (Peak #1) contained a protein with the same properties. (b, c) Analysis of ledodin by SDS-PAGE. Electrophoresis was carried out as indicated in Section 4, and then the gel was stained with Coomassie brilliant blue (b) or by a glycoprotein staining kit (c). The numbers indicate the corresponding size of the standards in kDa. (d) Effect of ledodin (closed circles) and peak #1 (open circles) on protein synthesis. Translation assays were carried out using a cell-free system, as indicated in Section 4. The effect of BE27, a RIP from *Beta vulgaris* (closed squares), is also represented. (e, f) rRNA N-glycosylase activity of ledodin in rabbit reticulocyte lysate (e) and mealworm (f) ribosomes compared to that of BE27. The rRNA N-glycosylase activity was tested as indicated in Section 4. Each lane contained 5 μg of RNA isolated from untreated (control) ribosomes or treated with the toxin. The arrows indicate the RNA fragment released as a result of the action of RIP after treatment with acid aniline (+). The numbers indicate the size of the markers (M) in nucleotides.

indicates that ledodin is an N-glycosylase that acts on the SRL of mammalian ribosomes. We performed the same assay on insect ribosomes and as shown in Figure 1f, BE27 released the diagnostic fragment from ribosomes of mealworm, while ledodin did not, indicating that insect ribosomes are insensitive to ledodin (Figure 1f). This represents a difference with respect to plant RIPs, since to

date all RIPs studied have been shown to be active against any type of animal ribosomes (Iglesias et al., 2016; Zhu et al., 2018). Many plant RIPs are active against fungal ribosomes, and some of them are active against bacterial ribosomes (Iglesias et al., 2016; Zhu et al., 2018). We assayed ledodin with yeast ribosomes and with ribosomes from *Micrococcus lysodeikticus*, but in

neither case was release of the diagnostic fragment observed (Figure S2). Although the SRL is conserved in all organisms, the binding of any RIP to the ribosome requires interaction with ribosomal proteins that are not conserved (Grela et al., 2019) Because of this, ribosomes present various sensitivities to the different RIPs (Girbés & Ferreras, 1998). This may explain the different sensitivity of ribosomes to the N-glycosylase action of ledodin. The fact that bacterial and yeast ribosomes are not sensitive to ledodin can be considered an advantage if this protein is to be cloned and expressed in the microorganisms most used for this purpose. Some plant RIPs are also able to remove more than one adenine from the 28S rRNA and many of them can depurinate not only rRNA but also other polynucleotide substrates such as DNA, poly(A), mRNA, tRNA, and viral RNA. Therefore, the name adenine polynucleotide glycosylase (APG) or polynucleotide: adenosine glycosylase (PNAG) has been proposed for RIPs (Barbieri et al., 1997; Iglesias et al., 2016). RIPs from plants display different APG activities on DNA and RNA. Some of them have low activity, while others, such as BE27 or the RIPs obtained from *Phytolacca dioica*, have very high activity. Ledodin possesses little or no activity on both DNA and different RNAs (Figure S3), when compared to BE27. The fact that ledodin does not have activity on insect and yeast ribosomes or on Tobacco Mosaic Virus RNA is very relevant, since among the roles attributed to RIPs from plants is that of being a defense agent against fungi, insects, and viruses, although not all RIPs are active against pathogens such as viruses and fungi (Citores et al., 2021; Iglesias et al., 2016; Zhu et al., 2018). Finally, some RIPs have been reported to display endonuclease (nicking) activity on supercoiled plasmid DNA producing relaxed or even linear plasmids (Iglesias et al., 2016). This ability may be necessary for these proteins to perform different biological functions, including resistance to viruses (Citores et al., 2021). Therefore, we have tested the ledodin endonuclease activity on the plasmid pCR2.1 compared to BE27. BE27 promoted the conversion of supercoiled pCR2.1 DNA into the relaxed form (Figure S4) as reported elsewhere (Iglesias et al., 2016). In contrast, ledodin did not promote such conversion even at a concentration fivefold higher than that used for BE27 (Figure S4).

### 2.3 | Cytotoxicity of ledodin

Although all plant RIPs are cytotoxic to a greater or lesser degree, they present very different  $IC_{50}$  values (concentration inhibiting 50% of protein synthesis, or 50% of viability) ranging from 0.3 pM to 34  $\mu$ M (Citores

et al., 2013). Consequently, they present very different  $LD_{50}$  values (dose that kills 50% of animals), ranging from 0.56  $\mu$ g/kg to 40 mg/kg of body weight (Citores et al., 2013). Some type 2 RIPs such as ricin are extremely toxic, whereas the toxicity of type 1 RIPs is lower, as they lack the lectin part and are therefore unable to bind to cells as type 2 RIPs do. The activity of ledodin in whole cells was studied by incubating HeLa and COLO 320 cells with different concentrations of ledodin for 72 h, after which cell viability was determined. Ledodin reduced the viability of HeLa cells, showing an  $IC_{50}$  of 90 nM (Figure 2a), similar to or lower than that of many type 1 RIPs (Citores et al., 2013). To investigate the capability of ledodin to reach the cytosol and inactivate the ribosomes after being endocytosed, we analyzed the ribosomal RNA from HeLa cells treated with ledodin for 72 h. Figure 2b shows that the ribosomes were depurinated, releasing the diagnostic fragment after treatment of the RNA with acid aniline. Interestingly, the same RNA fragment was obtained from HeLa cells incubated with the ribotoxin  $\alpha$ -sarcin, although in this case treatment of the RNA with aniline was not necessary since  $\alpha$ -sarcin is an endonuclease (Figure 2b). These results indicate that ledodin can enter HeLa cells and inactivate ribosomes through its N-glycosylase activity on the SRL of ribosomal RNA, thereby causing cell death. Furthermore, HeLa cells treated with ledodin showed apoptotic morphological features, such as cell rounding and blebbing (Figure S5) suggesting that the apoptotic pathway was implicated in the cell death mediated by ledodin, as already proved for other plant RIPs. On the other hand, COLO 320 cells were 300-fold less sensitive than HeLa cells (Figure 2a), which may be due to a lower endocytosis rate, or a different intracellular pathway, as has been reported for RIPs from plants (Citores et al., 2013). The rate of endocytosis and the intracellular pathway of the toxin depend mainly on the receptor it uses to internalize, and therefore the more the cell line expresses the target receptor the more sensitive it is to the toxin (Citores et al., 2013).

In addition, some plant RIPs display antifungal activity, that is, they are able to cross the plasma membrane of some fungal cells and, through their N-glycosylase activity, inactivate the ribosomes, killing the cells (Iglesias et al., 2016; Landi, Ragucci, et al., 2022). For this reason, an antifungal role has been attributed to some of these proteins and transgenic plants bearing RIP genes, that are resistant to fungal diseases, have been obtained (Zhu et al., 2018). Regarding fungal RIPs, the only one that presents such activity is lyophyllin, which shows N-glycosylase activity in yeast ribosomes (Lu et al., 2021) and exerts antifungal activity against *Physalospora piriicola* and *Coprinus comatus*, but not against *Rhizoctonia*

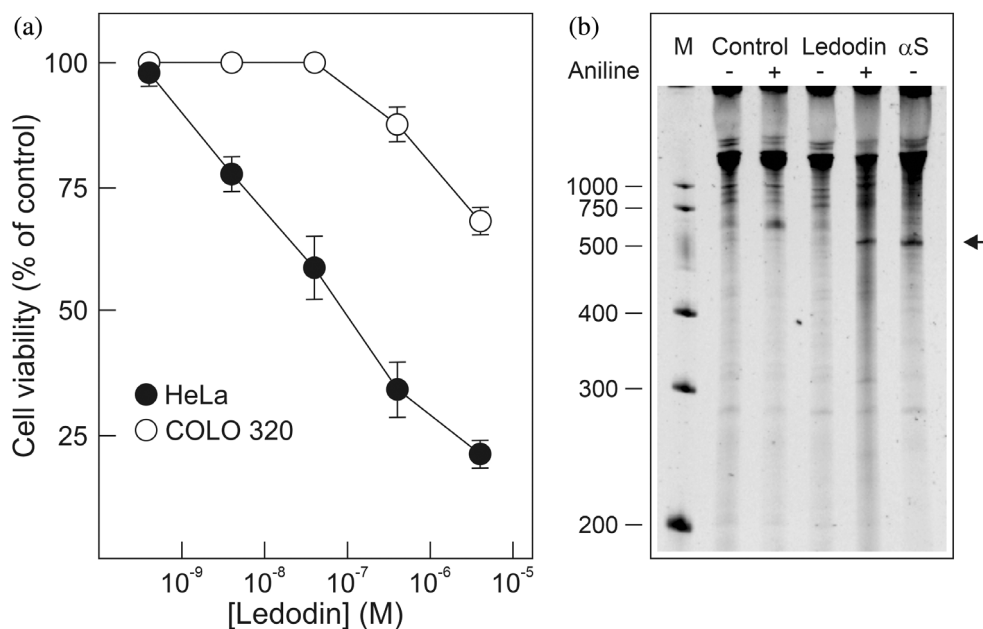


**FIGURE 2** Cytotoxicity of ledodin on HeLa and COLO 320 cells. (a) Effect of ledodin on the viability of HeLa (closed circles) and COLO 320 (open circles) cells. Cell viability was assessed by a colorimetric assay, as indicated in Section 4. Data represent the mean  $\pm$  SD of three experiments performed in duplicate. (b) rRNA N-glycosylase activity of ledodin on HeLa cells RNA. The rRNA N-glycosylase activity was evaluated as described in Section 4. Each lane contained 2  $\mu$ g of RNA isolated from untreated cells (Control) or cells incubated 72 h with 2  $\mu$ M of ledodin or 0.05  $\mu$ M of  $\alpha$ -sarcin ( $\alpha$ S). The arrow indicates the RNA fragment released as a result of toxin action after treatment with acid aniline (+), or the fragment released by  $\alpha$ -sarcin. The numbers indicate the size of the standards (M) in nucleotides.

*solani*, *Mycosphaerella arachidicola*, and *Colletotrichum gossypii* (Lam & Ng, 2001). This is not the case of ledodin, which, consistent with the result obtained with yeast ribosomes, had no effect on the growth of the fungus *Penicillium digitatum* at a concentration of 40  $\mu$ g/mL, whereas 1  $\mu$ g/mL of  $\alpha$ -sarcin or 15  $\mu$ g/mL of BE27 inhibited fungal growth by 94% and 74%, respectively (Figure S6).

The results of enzymatic activities and cytotoxicity provide some evidence about the biological role of ledodin. Based on these types of activities, defense roles for RIPs and ribotoxins such as antiviral, antifungal, insecticidal, or antifeedant defense against herbivores, have been proposed (Zhu et al., 2018). The former seems ruled out for ledodin, but the latter could be, since enough ledodin (at least 2.7 mg per 100 g of fresh tissue) has been obtained from shiitake fruiting bodies to have toxicity to herbivores that consume them. On the other hand, part of the toxicity attributed to these mushrooms when consumed raw or undercooked could be due to this protein.

## 2.4 | Sequence of ledodin

To obtain information on the identity and structure of ledodin, its N-terminal sequence was obtained by Edman degradation (Figure 3). Subsequently, the result was used

to search for similar sequences using BLAST in the NCBI database. The sequence matched the sequence with accession number KAF8826020.1, obtained by conceptual translation from the genome of *Lentinula edodes* (GenBank: JABFYJ000000000.1). Considering this sequence and the amino terminal sequence obtained by Edman degradation, specific primers were designed for the amplification of ledodin cDNA (see Section 4.12). A PCR fragment of about 600 bp was obtained (Figure S7) and cloned into the pCR<sup>TM</sup>II vector. Seven clones were sequenced and two of them had a sequence consisting of 603 bp, whereas the remaining five had a 659-bp sequence that was identical to the above but containing a 56-bp intron (Figure 3a). As previously reported, intron retention in the mature mRNAs might be related to some kind of regulation (Monteuuis et al., 2019).

The amino acid sequence deduced from the intronless cDNA sequence was used to map ledodin by enzymatic (trypsin) and chemical (CNBr) hydrolysis of the protein, determining the molecular masses of both peptides and fragments in mixtures by MALDI-ToF MS analysis (Table S1), which were superimposed on the amino acid sequence (Figure 3b). The sequence of the tryptic peptides obtained provided 95% of the amino acid sequence deduced from the cDNA sequence (191 of 201). The C-terminal region can be confirmed by the presence of the lysinyl residue at the C-terminal position of T-11 and the

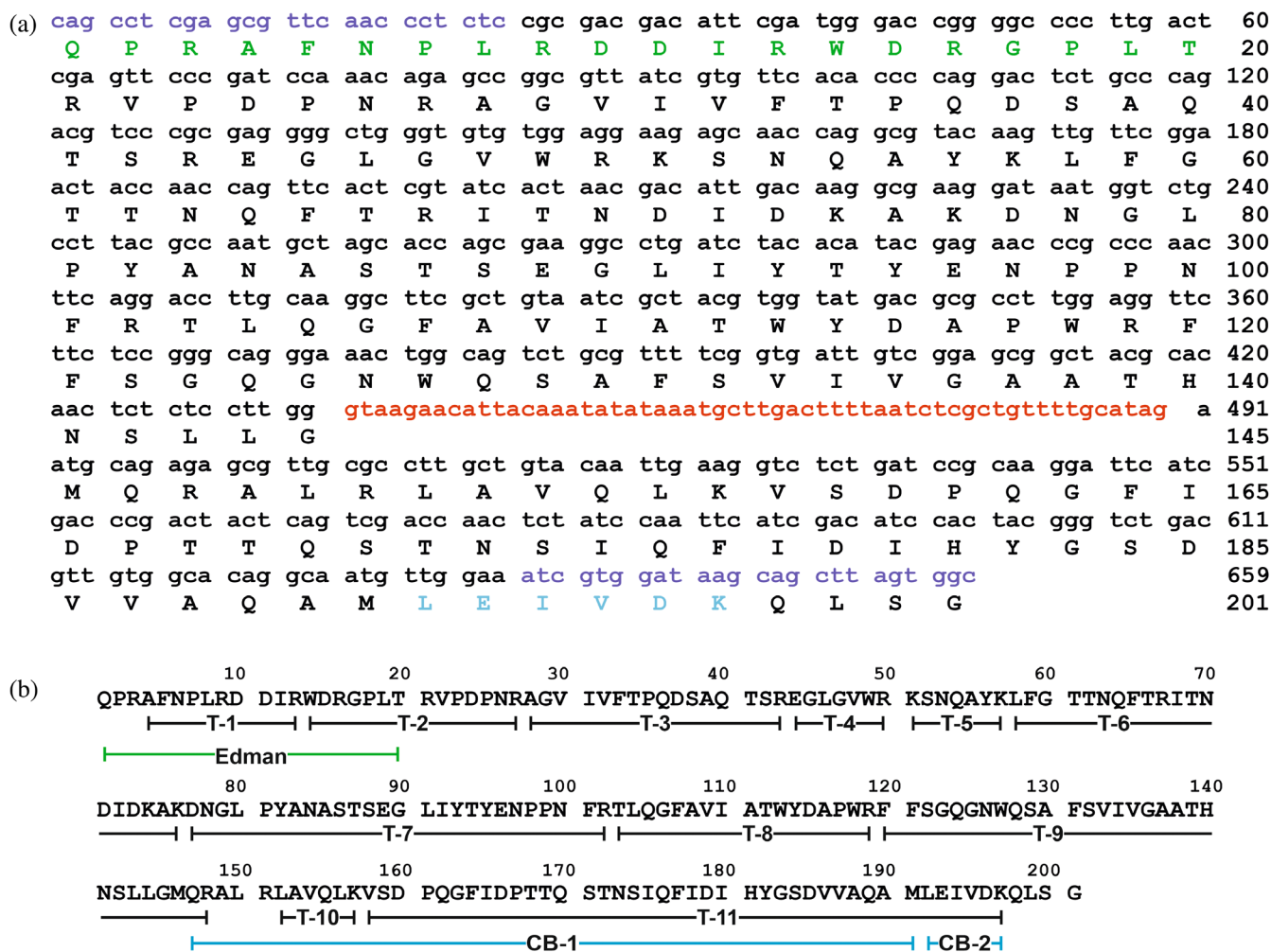


**FIGURE 3** Full-length sequence and derived amino acid sequence of the ledodin gene. (a) The sequence of cDNA from ledodin was obtained as indicated in Section 4. The sequences that correspond to primers and intron are represented in blue and red, respectively. The amino terminal sequence obtained by Edman degradation and the terminal carboxyl sequence obtained by cyanogen bromide treatment and mass spectrometry are represented in green and cyan in the amino acid sequence, respectively. (b) Mapping of ledodin with trypsin and cyanogen bromide. The tryptic (T-) and chemical (CB-) fragments determined by MALDI-ToF mass spectrometry are shown in Table S1, and the amino terminal sequence obtained by Edman degradation are superimposed with the deduced sequence from cDNA.

absence of the extra QLSG tetrapeptide in the C-terminal region of the reference sequence (see Figure 3b). No tryptic peptides were mapped on the first 19 amino acid residues of the sequence KAF8826020.1, suggesting that this sequence is not present in the mature protein. This finding confirms Edman sequencing results. To complete the C-terminal region, ledodin was subjected to chemical hydrolysis with CNBr. From analysis of the fragment mixture by MALDI-ToF MS, two fragments mapping the C-terminal region were found (CB-1, position 147–191; and CB-2, position 192–197; Table S1). In particular, CB-2 confirms that the C-terminal structure of ledodin consists of a lysinyl residue without the tetrapeptide QLSG, thus absent in the structure of mature ledodin. This strategy, together with Edman's degradation, allowed mapping the entire sequence of the mature ledodin.

Regarding the sequence KAF8826020.1, ledodin presents three differences: the absence of 19 amino acids at the N-terminal region and 4 at the C-terminal region, and the change of glycine 115 by aspartic acid. The first two differences could be due to proteolytic processing of a precursor.

## 2.5 | Prediction of the structure of ledodin

The structure of ledodin was predicted using AlphaFold2 (Jumper et al., 2021) and RoseTTAFold (Baek et al., 2021) programs. As can be seen in Figure 4a, despite using different algorithms the two programs predicted almost identical structures. The greatest differences between the two predictions occurred in the loops

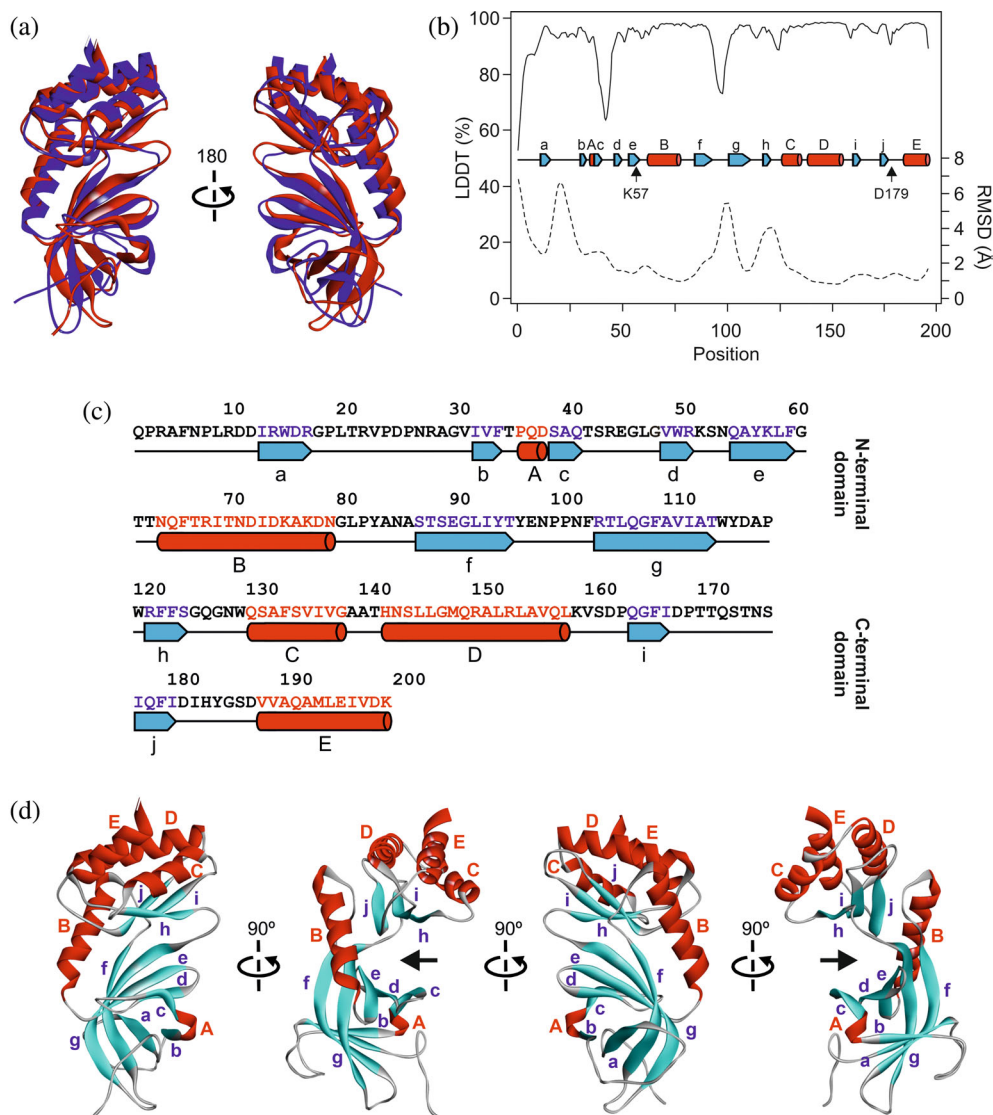


**FIGURE 4** Prediction of the three-dimensional structure of ledodin. (a) Comparison of ledodin structure predictions performed by AlphaFold2 (red) and RoseTTAFold (blue). (b) Confidence of the models predicted by AlphaFold2 and RoseTTAFold. The local distance difference test (LDDT) performed by AlphaFold2 (solid line) and the root-mean-square deviation (RMSD) performed by RoseTTAFold (dashed line) for each position in the polypeptide chain of the protein are represented. The inset indicates the secondary structure (blue ribbons,  $\beta$  strands; red cylinders,  $\alpha$  helices; lines, coils) of each position predicted by AlphaFold2. Arrows indicate the position of K57 and D179. (c) The secondary structures of ledodin are shown in red ( $\alpha$  helices, labeled from A to E) and blue ( $\beta$  chains, labeled from a to j). (d) Three-dimensional structure of ledodin predicted by AlphaFold2. The  $\alpha$  helices (red), the  $\beta$  chains (cyan), and the coils (gray) are represented. The helices are labeled A to E and the  $\beta$  strands are labeled a-j. Arrows indicate the putative active site pocket

of the amino terminal region, while the two predictions agree in the structures of the helices and  $\beta$ -chains (Figure 4a). Both models showed excellent confidence indices, with LDDT values above 90% for the AlphaFold model and RMSD values below 2 Å for the RoseTTAFold model (Figure 4b). This allows these models to be used for studies at the molecular level (Baek et al., 2021; Jumper et al., 2021). The exception were the amino-terminal end and the loops between some of the  $\beta$ -chains (i.e., a-b, c-d, and f-g, Figure 4b).

Ledodin shows a globular structure with two clearly differentiated domains (Figure 4c,d). The amino terminal

domain includes the first 117 amino acids and consists mainly of seven  $\beta$  chains (a-g) arranged in a small barrel. Chains b and c are connected by an helix of three amino acids (helix A) and between the e and f chains is an  $\alpha$  helix (helix B) formed by 16 amino acids. The carboxyl terminal domain includes the other 80 amino acids and consists of three  $\beta$  chains and three  $\alpha$  helices that with an hCDijE order give rise to a two-layer alpha/beta sandwich (Figure 4c,d). Between the two domains, a deep cleft can be distinguished, which appears to be a good candidate to host the active site (Figure 4d, arrows). It is noteworthy that two amino acids (lysine 57 and aspartic



acid179) which, as will be discussed later could be involved in catalysis, are found in this pocket and exhibit very high LDDT values (96% and 94%, respectively) and very low RMSD values (1.53 and 1.37 Å, respectively; Figure 4b, arrows).

## 2.6 | Putative active site of ledodin

RIPs present an active site in which five amino acids are conserved: three amino acids (two tyrosines and one tryptophan) that contribute to adenine binding, and two amino acids (glutamic acid and arginine) that participate in catalysis (Di Maro et al., 2014). The mechanism of catalysis is not fully elucidated but is similar to that of monofunctional DNA N-glycosylases (Drohatsky & Maiti, 2014). As discussed above, the confidence indices obtained in the prediction of ledodin structure allow, with appropriate caveats, studies at the molecular level. Because adenosine monophosphate (AMP) has been used to study the active site of some RIPs by crystallography and X-ray diffraction (Guo et al., 2003), we have used this ligand to perform an *in silico* study to identify the potential active site of ledodin. To locate the active site, we

carried out a blind docking with AMP using the AutoDock 4.2 program whose solutions targeted the pocket between the two domains of the protein (see Figure 4d, arrows). As indicated in Section 4, two successive refinements were made focusing on this pocket and better values of estimated free energy of binding were obtained. The best solution is shown in Figure 5a, in which the glutamic acid and arginine characteristic of RIPs were not found, but lysine (K57) and aspartic (D179) that are characteristic of many DNA N-glycosylases were found (Hitomi et al., 2007). In order to elucidate whether lysine 57 plays a role in catalysis, we decided to perform a treatment of ledodin with succinimidyl 3-(2-pyridyldithio)propionate (SPDP), which has been used to quantify lysinyl residues at the functional sites of enzymes (Hacker et al., 2017). The compound SPDP is specific for primary amino groups ( $\epsilon$ -NH<sub>2</sub> group of lysines or protein N-terminal -NH<sub>2</sub> group). We compared the rRNA N-glycosylase activity of the SPDP-treated and untreated protein, finding that the treatment inactivated ledodin (Figure 5b). Such treatment did not affect the RIP quinoin because, although many lysinyl residues are found in RIPs, none of them participate in catalysis. However, to experimentally identify the modified lysinyl residue, a

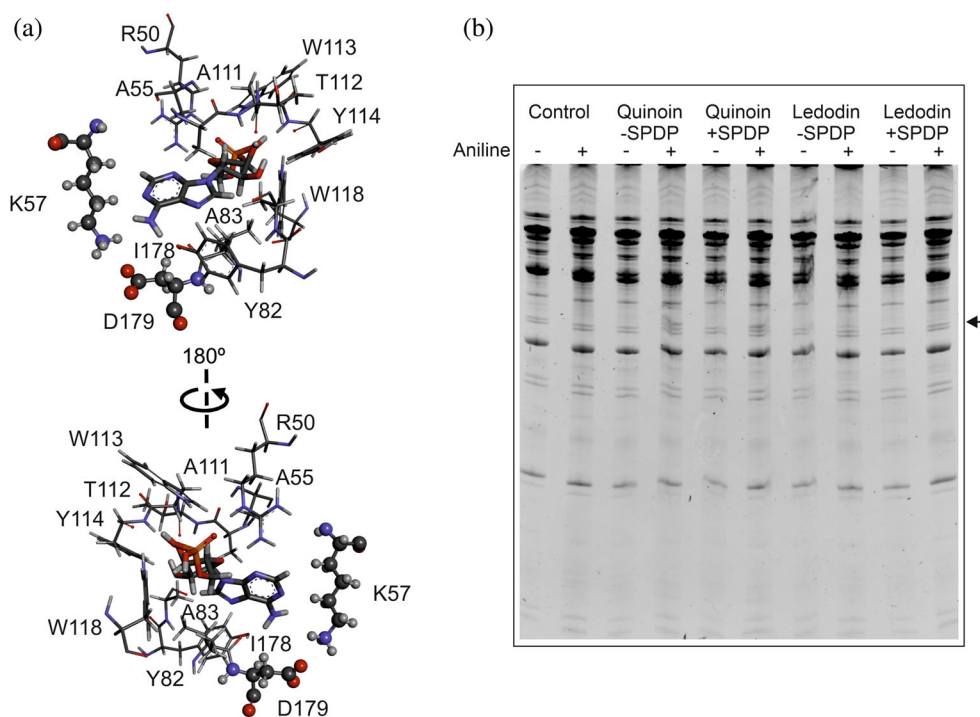


**FIGURE 5** Prediction of the active site of ledodin and the mechanism of catalysis. (a) Three-dimensional model of the AMP-binding site from ledodin. The amino acids that bind the AMP molecule (thick sticks) by either  $\pi$  interactions or hydrogen bonds are represented by thin sticks. The putative catalytic amino acids lysine and aspartic acid are represented by balls and sticks. (b) rRNA N-glycosylase activity of ledodin and quinoin on rabbit ribosomes, with (+SPDP) and without (-SPDP) chemical modification by SPDP. rRNA N-glycosylase activity was assayed as indicated in Section 4. Each lane contained 3  $\mu$ g of RNA isolated from either untreated (control) or toxin treated rabbit reticulocyte lysate ribosomes. The arrow indicates the RNA fragment (Endo's fragment) released as a result of toxin action after acid aniline treatment (+); (-) without aniline treatment.

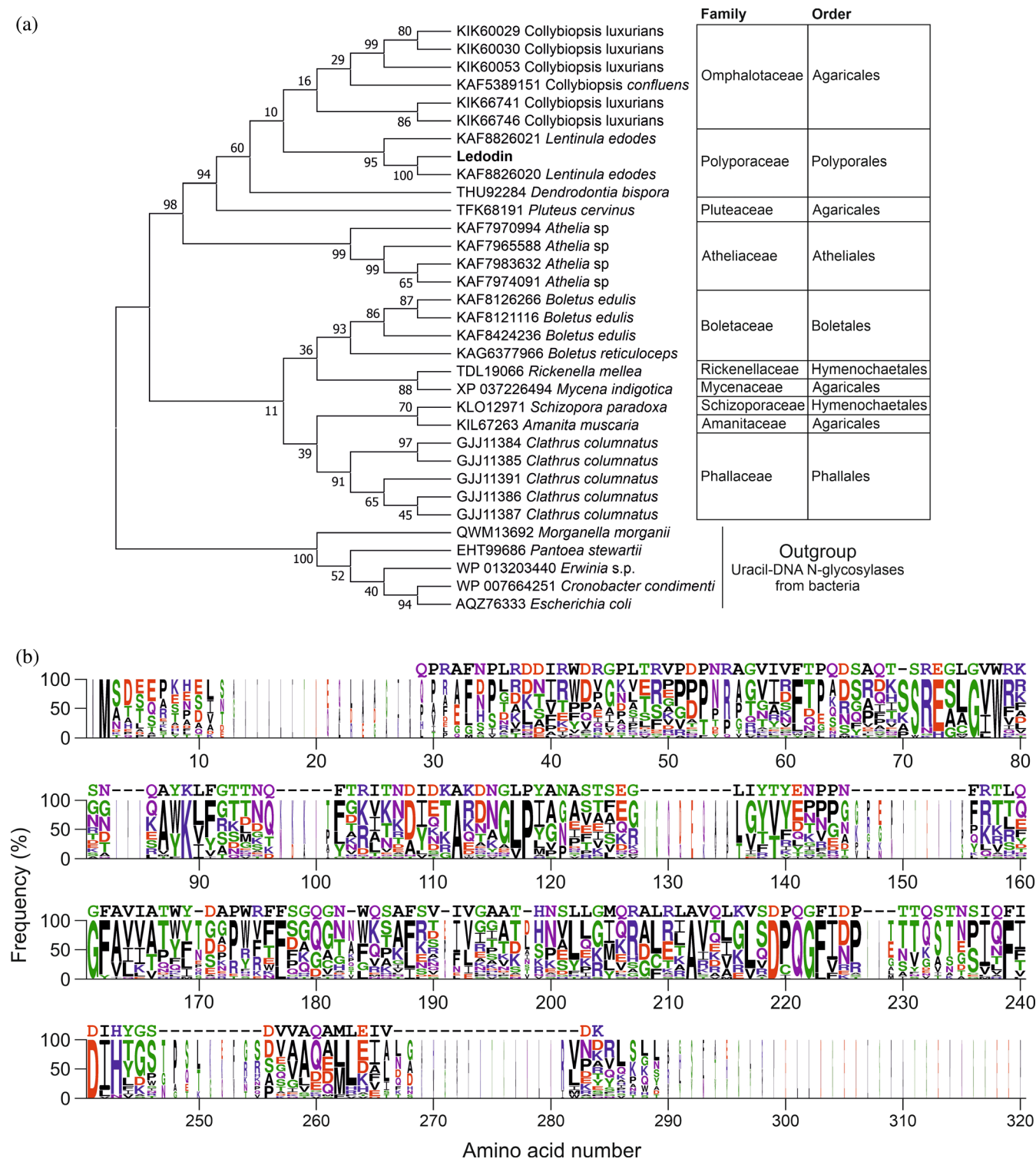


**FIGURE 6** Alignment and phylogenetic relationship of ledodin with amino acid sequences of hypothetical proteins derived from the genomes of various Agaricomycetes. (a) Molecular phylogenetic analysis by the Maximum Likelihood method of ledodin and hypothetical proteins from genomes of various Agaricomycetes. Evolutionary history was inferred as indicated in Section 4. The percentage of trees in which the associated taxa are grouped is shown next to the branches. The species and access number are indicated. (b) The sequence logo representation of the alignment of the sequences of the panel A was created as indicated in Section 4. Letter height is proportional to the frequency of that amino acid at that position in the alignment respect to all the amino acids; letter width is proportional to the frequency of that amino acid but including gaps. The ledodin sequence is represented above the logo. Colors indicate amino acid classes according to chemical properties: hydrophobic (black), polar (green), neutral (purple), acidic (red), basic (blue).

mapping of peptides obtained after endoproteinase Glu-C digestion from ledodin with and without SPDP treatment was carried out as previously reported (Delforge et al., 1997). The MALDI-ToF MS analysis of peptides mixture obtained by ledodin endoproteinase Glu-C digestion with or without SPDP treatment showed the presence of different peptides. In particular, peptides mixture without chemical modification revealed the presence of an experimental molecular mass of 4993.60 ( $[M + H]^+$ ) Da, mapping the sequence position 45–89 (theoretical mass 4993.50 ( $[M + H]^+$ ));  $_{45}\text{-GLGVWRKSNQAYKLF GTTNQFTRITNDIDKAKDNGLPYANASTSE}_{-89}$ ; ( $\Delta_{\text{mass}} = 0.10$ ) Da, while this peptide mass was absent in ledodin peptides mixture with chemical modification (data not shown). On the other hand, a novel peptide mass of 5191.01 ( $[M + H]^+$ ) Da was detected after chemical modification. This peptide mapped the position 45–89 of ledodin considering an additional molecular mass of 197.29 Da, corresponding to the chemical modification of a single lysinyl residue in the presence of SPDP. However, this peptide contains four lysinyl residues (K51, K57, K74, and K76); thus, to identify the reactive lysinyl residue, the mixture of Glu-C peptides was further digested with trypsin. The chemical modified peptides mixture after subdigestion revealed an experimental molecular mass of 2200.26 ( $[M + H]^+$ ) Da absent in peptides mixture without chemical treatment (Figure S8). This molecular mass mapped the position 51–67 ( $_{51}\text{-KSNQAYKLF GTTNQFTR}_{-67}$ ; theoretical molecular mass 2004.03 ( $[M + H]^+$ ) Da) considering an additional mass of 197.29 Da (theoretical molecular mass 2201.32 Da;  $\Delta_{\text{mass}} = 1.06$  Da), corresponding to the reaction between a lysinyl residue and the SPDP. The tryptic peptide in position 51–67 contains two lysinyl residues: K51 susceptible to tryptic cleavage (lysinyl residue accessible to trypsin) and K57 missed cleavage (inaccessible to trypsin). These results suggest that the lysinyl residue that reacted with SPDP is K57, which is in agreement with the prediction obtained by molecular docking.

In summary, the above suggests that the catalytic mechanism of ledodin would be one of the two proposed for RIPs and DNA N-glycosylases (Drohat & Maiti, 2014), but the active site would be more closely related to that of some DNA N-glycosylases (Hitomi et al., 2007) than to that of RIPs (Di Maro et al., 2014).

## 2.7 | Homology of ledodin with other hypothetical proteins

By using ledodin sequence, a database search yielded 40 hits, all of them unknown protein sequences obtained by conceptual translation of Agaricomycetes genomes.

From them, we have selected the 27 that most closely resemble ledodin in size and that are shown in Figure 6a. The closest in the phylogenetic tree are two hypothetical protein sequences from shiitake. The sequence with accession number KAF8826020 is almost identical to ledodin, changing only one amino acid (D115G) and having 19 and 4 extra amino acids at the amino and carboxyl terminus, respectively. These latter differences are probably due to processing of the precursor. The protein KAF8826021 from *Lentinula edodes* has an identity of 88.18% with KAF8826020 and it is noteworthy that, similar to ledodin, it also contains aspartic acid instead of glycine. From the others, the closest are those of the genus *Colybiopsis*, with identities from 47.45% to 74.62%. As shown in Figure 6a, homologous sequences also exist in different orders of Agaricomycetes (Agaricales, Polyporales, Atheliales, Boletales, Hymenochaetales, and Phallales), suggesting that this type of protein toxin could be widely distributed in the division Basidiomycota (or at least in the class Agaricomycetes). It is also worth mentioning that some of these species are edible therefore, this type of protein could represent a certain risk for some people, as is the case of shiitake. Figure 6b shows a logo representing the alignment of the 27 sequences of Figure 6a. There are 12 invariant amino acids: G76, W78, K89, A112, P118, G161, A212, D219, Q221, G222, F239, and D241, which correspond to amino acids G47, W49, K57, A75, P81, G106, A153, D169, Q162, G163, F177, and D179 of ledodin. As discussed above, K57 and D179 could be the catalytic amino acids, the rest could play critical roles in the active site or the whole protein structure.

## 3 | CONCLUSIONS

The fruiting bodies of shiitake (*Lentinula edodes*) contain a large amount of a cytotoxic protein that we have named ledodin. This protein strongly inhibits protein synthesis in a cell-free rabbit reticulocyte lysate system. It possesses N-glycosylase activity on the sarcin-ricin loop (SRL) of the 28S rRNA of mammalian ribosomes, which links it to ribosome-inactivating proteins (RIPs) from plants. However, it is inactive against insect, fungal and bacterial ribosomes. Unlike many RIPs, ledodin does not possess significant adenine polynucleotide glycosylase or DNA nicking activities. In silico studies predict that it is a globular protein with two domains, an amino-terminal domain with a small beta-barrel structure and a carboxyl-terminal domain with a two-layer alpha/beta sandwich structure; between the two domains is the active site that presents a lysine and a glutamic acid as catalytic amino acid candidates. The sequence and structure of ledodin are not related to any protein with a known function, but

a preliminary database search has revealed that other fungi have homologous proteins in their genome, therefore, ledodin could be the first of a family of toxins present in a considerable number of fungi of the class Agaricomycetes, some of them edible. The discovery of a new family of cytotoxic proteins in mushrooms is of great interest in health, both for its implication in food safety and for its potential applications in biomedicine and biotechnology. Regarding the latter, it has great potential to be used as a substitute for proteins with a similar target (ricin, saporin,  $\alpha$ -sarcin, diphtheria toxin) for the construction of immunotoxins, conjugates, engineered proteins, or nanocapsules for the experimental therapy of cancer or viral diseases.

## 4 | MATERIALS AND METHODS

### 4.1 | Materials

The fruiting bodies of shiitake, *Lentinula edodes* (Berk.) Pegler, from the company Hongos Fernández Guridi (Pradejón, La Rioja, Spain) and the mealworms (*Tenebrio molitor* L.) were bought at local markets. The strain of *Penicillium digitatum* (Pers.) Sacc. was isolated in our laboratory and typified by the Spanish Type Culture Collection (CECT), Valencia, Spain. BE27 was isolated following a procedure described previously (Iglesias et al., 2015). The sources of the chemicals were described previously (Iglesias et al., 2017). Bovine pancreatic ribonuclease A (RNase A) and yeast RNA were purchased from Roche Diagnostics S.L. (Barcelona, Spain). SP-Sepharose was purchased from GE Healthcare (Barcelona, Spain). Endoproteinase Glu-C and trypsin TPCk-treated (sequencing grade) were purchased from Merck Life Science S.r.l. (Milan, Italy). HPLC grade solvents were obtained from Merck (VWR International S.r.l., Milan, Italy). Cyanogen bromide (CNBr) was obtained from Fluka (Milan, Italy). SPDP (succinimidyl 3-(2-pyridyldithio) propionate) was purchased from Thermo Fisher Scientific (Rodano, Milan, Italy). Century™-Plus RNA Markers were purchased from Fisher Scientific (Madrid, Spain). Potato dextrose agar and Potato dextrose broth media were purchased from Sigma-Aldrich (Madrid, Spain).

### 4.2 | Cell lines and culture

COLO 320 (human colon carcinoma) and HeLa (human cervix epitheloid carcinoma) cells, were obtained from the European Culture Collection (ECACC) and grown in RPMI 1640 medium (GIBCO BRL, Barcelona, Spain)

supplemented with 10% fetal bovine serum (FBS), 100 U/mL penicillin and 0.1 mg/mL streptomycin under 5% CO<sub>2</sub> at 37°C.

### 4.3 | Purification of ledodin

One hundred grams of fresh fruiting bodies of shiitake were ground with a blender and extracted overnight at 4°C with eight volumes of PBS (140 mM NaCl, containing 5 mM sodium phosphate, pH 7.5). The extract was clarified by filtering it through a nylon mesh and then centrifuged for 30 min at 9000 rpm in a JA-10 rotor (14,300g) at 2°C. Glacial acetic acid was added to the supernatant until a pH of 4.0 was reached, after which it was clarified again by filtering and centrifuging it under the same conditions. The acidified extract was subjected to ion exchange chromatography in a column of SP-Sepharose Fast Flow (i.d. 5 × 8 cm, 157 mL) equilibrated in 10 mM sodium acetate (pH 4.5) at 8.5 mL/min flow rate. After sample loading, the column was washed with 10 mM sodium acetate (pH 4.5), and then with 5 mM sodium phosphate (pH 6.66). The column was eluted with 0.5 M NaCl in the same buffer and the eluted protein (17.5 mg of protein in 120 mL) was dialyzed three times against 4 L of water at 5°C. Sodium phosphate (pH 6.66) was added to a concentration of 5 mM and the resulting sample was subjected to chromatography in a column of SP-Sepharose Fast Flow (i.d. 1 × 7.5 cm, 5.9 mL) equilibrated in 5 mM sodium phosphate (pH 6.66) at a flow rate of 1 mL/min and eluted with 40 volumes of a linear gradient of 0–200 mM NaCl in the same buffer. Fractions containing ledodin (2.7 mg of protein in 10 mL) were pooled and dialyzed against water (three times in 4 L of water at 5°C), lyophilized in 0.15 mg aliquots and stored at –20°C until use.

### 4.4 | Analytical procedures

Protein concentrations were determined using a spectrophotometric method (Iglesias et al., 2015). The homogeneity of the isolated protein was determined by SDS-PAGE with a Mini-Protean II mini-gel device (Bio-Rad; Milan, Italy), using 6% stacking (wt/vol) and 15% separation (wt/vol) gels under reducing conditions. Glycosylation analysis was performed on the gel after SDS-PAGE using Pro-Q Emerald 300 Glycoprot Probes Kombo (Life Technologies, Italy). The glycosylated proteins were visualized by the ChemiDoc™ XRS system. The amino terminal end of ledodin was sequenced by using automated Edman degradation performed on a Procise 494 sequencer (Applied Biosystems, Inc., Foster City, CA, USA) at the

Service of Protein Chemistry at the Margarita Salas Center for Biological Research (CIBMS, Madrid, Spain).

#### 4.5 | Assays of cell-free protein synthesis

The effect of ledodin on protein synthesis was determined through a coupled transcription-translation *in vitro* assay using a rabbit reticulocytes lysate system as described elsewhere (Iglesias et al., 2022). The data represent the average of five experiments in duplicate.

#### 4.6 | Ribonuclease activity

RNase activity was assayed using methylene blue (Iglesias et al., 2015). An RNA solution was prepared by dissolving 10 mg of yeast RNA in 10 mL of Mops buffer (0.1 M Mops-HCl, pH 7.5, 2 mM EDTA). The methylene blue buffer was prepared by dissolving 0.1 mg of methylene blue in 10 mL of Mops buffer. Then, 20  $\mu$ L of the RNA solution was mixed with 980  $\mu$ L of the methylene blue buffer and 20  $\mu$ L of water, ledodin, or RNase A. The samples were incubated at room temperature and the decrease in absorbance at 688 nm was monitored at 15, 30, 45, and 60 min.

#### 4.7 | rRNA N-glycosylase assays

rRNA N-glycosylase assays on rabbit reticulocyte, mealworm, yeast, and bacterium lysates and HeLa cells were conducted as described elsewhere (Iglesias et al., 2017, 2022).

#### 4.8 | Adenine polynucleotide glycosylase assays

Adenine polynucleotide glycosylase (APG) activity on salmon sperm DNA and N-glycosylase activity on polyribonucleotides (poly(A) and poly(G)) was measured according to the method reported elsewhere (Iglesias et al., 2016) with a few modifications. Either 10  $\mu$ g of salmon sperm DNA, 100  $\mu$ g poly(A) or 100  $\mu$ g poly(G) were incubated with 10  $\mu$ g of toxin in 300  $\mu$ L of a reaction mixture which contained 100 mM KCl, 50 mM magnesium acetate (pH 4), at 30°C for 2 h. After incubation, polynucleotides were precipitated with ethanol at -80°C overnight and centrifuged at 13,000 rpm for 15 min. Nucleobases released from toxin-treated polynucleotides were determined in the supernatants spectrophotometrically at 260 nm. The APG activity on tobacco mosaic

virus (TMV) RNA was carried out as described elsewhere (Iglesias et al., 2016).

#### 4.9 | DNA cleavage experiments

Nicking activity experiments were performed as previously reported (Iglesias et al., 2016). Each reaction contained 5  $\mu$ g of toxin and 200 ng of pCR2.1 DNA in a final volume of 10  $\mu$ L of 10 mM Tris-HCl, 5 mM MgCl<sub>2</sub>, 50 mM NaCl and 50 mM KCl, pH 7.8. Samples were incubated for 2 h at 30°C, run on agarose gel (0.8%) in TAE buffer (0.04 M Tris, 0.04 M acetate, 1 mM EDTA, pH 8.0) and visualized by Gel Red nucleic acid staining (Biotium, Inc., Hayward, CA).

#### 4.10 | Cell viability assays

Cell viability was determined with a colorimetric assay based on cleavage of the tetrazolium salt WST-1 to formazan by mitochondrial dehydrogenases in viable cells, as described elsewhere (Iglesias et al., 2022).

#### 4.11 | Antifungal activity measurements

The growth inhibition assays of ledodin against *P. digitatum* were performed in 96-well microtiter plates as described elsewhere (Iglesias et al., 2016).

#### 4.12 | Synthesis of cDNA, cloning, and sequence

A portion of the fresh fruit body of shiitake (100 mg) was disrupted using mortar and pestle and grinded to a fine powder under liquid nitrogen, and total RNA was isolated using the RNeasy Minikit (Qiagen, Barcelona, Spain) according to the manufacturer's instruction. Poly(A)-rich RNA was reverse transcribed using the synthetic oligonucleotide T1 (5' CGTCTAGAGTCGAC-TAGTGC[T]20 3'). Approximately 1  $\mu$ g of total RNA and 1  $\mu$ L of RNase inhibitor were incubated at 65 °C in a thermal cycler for 5 min. It was later cooled on ice for 1 min and 15  $\mu$ L of reaction mixture containing: 1 $\times$  PCR Buffer II, 5 mM of MgCl<sub>2</sub>, 1 mM of each dNTP, 10  $\mu$ M of T1, and 2.5 U/ $\mu$ L of MuLV reverse transcriptase (RNA PCR kit Roche, Roche Diagnostics SL, Sant Cugat del Vallès, Barcelona, Spain) was added. The reaction mixture was incubated for 20 min at 23°C, then for 20 min at 42°C, and finally 5 min at 99°C. The specific primers for the ledodin gene sequence were designed and synthesized

based on the N-terminus (obtained by Edman degradation) and the KAF8826020 sequences: LE-F1 as forward primer (5' CAGCCTCGAGCGTTCAACCCTCTC 3'), and LE-R1 as reverse primer (5' GCCACTAAGCTGCTTATCACGAT 3'). For cDNA amplification, 0.2  $\mu$ L of the above synthesized cDNA were used and 18.8  $\mu$ L of master mix (1 $\times$  PCR buffer/Mg<sup>2+</sup>, 0.2 mM dNTPs mix, 2.5 U Taq Polymerase [Invitrogen, Madrid, Spain] and 0.5  $\mu$ M of each primer) were added. PCR amplification was done with the following conditions: an initial denaturation at 94°C for 3 min, followed by 35 cycles of 94°C for 30 s, 55°C for 60 s and 72°C for 60 s, and an additional extension of 10 min at 72°C. About 5  $\mu$ L of amplified products was analyzed on 0.8% agarose gel. An amplicon of expected size (about 600 bp) was obtained, and the PCR product was purified using the NucleoSpin Gel and PCR Clean-up kit (Macherey-Nagel, Düren, Germany), according to the manufacturer's instruction. The purified PCR fragment was ligated into the pCR<sup>TM</sup>II vector and then was used to transform the Chemically Competent *Escherichia coli* INV $\alpha$ F' (Invitrogen-Thermo Fisher Scientific, Alcobendas, Spain) according to the manufacturer's instructions. Seven clones were purified and sequenced using M13 primers. DNA sequencing was carried out on the CENIT Support system (Villamayor, Salamanca, Spain). The DNA sequence for ledodin was submitted to GenBank (accession number: OP822047).

#### 4.13 | Ledodin cleavage and MALDI-ToF MS analysis

For structural studies, reverse phase (RP)-HPLC on a C-4 column (i.d. 4.6  $\times$  150 mm; Alltech, Sedriano, Milan, Italy) was used in order to desalt the protein, applying a linear gradient of 0.1% trifluoroacetic acid (TFA) and acetonitrile containing 0.1% TFA, from 5% to 65%, over 60 min, at a flow rate of 1 mL/min, monitoring the absorbance both at 214 and 280 nm (Di Maro et al., 1999). Desalted ledodin (50  $\mu$ g) was digested with trypsin, in 50 mM ammonium carbonate, pH 8.0, containing 10% acetonitrile. The enzyme was added in three steps (1:200; 1:100, and 1:50) with a final enzyme-to-substrate ratio of 1:50 (wt/wt) and the reaction was carried out at 37°C for 16 h (Ragucci et al., 2019). Chemical fragmentation with cyanogen bromide (CNBr) was carried out in 70% TFA to minimize adduct formations in presence of formic acid, as described (Landi et al., 2019). Mixture aliquots (1  $\mu$ L) of both tryptic digestion (T-) or chemical (CNBr) fragmentation (CB-) were mixed (1:1; vol:vol) with saturated  $\alpha$ -cyano-4-hydroxycinnamic acid matrix solution (10 mg/mL in acetonitrile/water [1:1, vol/vol], containing 0.1% TFA) and spotted onto a matrix-assisted laser

desorption ionization-time of flight (MALDI-ToF) micro MX (Waters, Milford, MA, USA) target plate. Samples were air-dried and then loaded into the mass spectrometer (Landi et al., 2019). Peptide spectra were collected in positive ion reflectron mode with the settings: source voltage, 12 kV; pulse voltage, 1999 V; detector voltage, 5200 V; and reflectron voltage, 2350 V. Measurements were performed in the mass range  $m/z$  500–5000 with a suppression mass gate set to  $m/z$  500. The instrument was externally calibrated using a tryptic alcohol dehydrogenase digest (Waters, Milford, MA, USA) as standard. Intact protein spectra were acquired in positive ion linear mode, by using a pulse voltage of 1200 V. A four-point external calibration was applied by using an appropriate mixture (10 pmol/ $\mu$ L) of insulin, cytochrome c, horse b and trypsinogen as standard proteins (Merk Life Science S.r.l.; Ragucci et al., 2019).

#### 4.14 | Chemical modification with SPDP

Protein inactivation by SPDP was performed at a protein concentration of 1 mg/mL in phosphate buffered saline with EDTA (100 mM sodium phosphate, 150 mM NaCl, 1 mM EDTA) pH 7.5. Ledodin (450  $\mu$ g) was incubated with SPDP in a 1:5 molar ratio and the reaction was carried out at 25°C for 30 min. In the pH condition used, the chemical modification with SPDP is specific for primary amino groups (i.e.,  $\epsilon$ -NH<sub>2</sub> group of lysinyl residue or NH<sub>2</sub> at N-terminal). The sample was desalted with Sephadex G-25 column and the loss of rRNA N-glycosylase activity of the modified protein (Ledodin-SPDP) was checked in a rabbit reticulocyte lysate system as previously reported (Iglesias et al., 2017, 2022). Not modified protein (ledodin) was used as control in the same conditions without SPDP. Subsequently, both ledodin and ledodin-SPDP (each 100  $\mu$ g) were desalted by RP-HPLC (see above) and then subjected to enzymatic digestion with Glu-C. Ledodin (~50  $\mu$ g) was digested with Glu-C in 50 mM ammonium carbonate, pH 8.0, containing 10% acetonitrile. The enzyme was added in three steps (1:100; 1:50, and 1:25) with a final enzyme-to-substrate ratio of 1:25 (wt/wt) and the reaction was carried out at 25°C for 16 h. Subdigestion of Glu-C peptides mixtures of ledodin with or without SPDP was carried out with trypsin.

#### 4.15 | Prediction of the structure of ledodin

The prediction of ledodin structure was carried out with the AlphaFold2 software (Jumper et al., 2021) following the instructions of the website <https://colab.research>.

[github.com/github/sokrypton/ColabFold/blob/main/AlphaFold2.ipynb#scrollTo=G4yBrceuFbf3](https://github.com/sokrypton/ColabFold/blob/main/AlphaFold2.ipynb#scrollTo=G4yBrceuFbf3) (accessed September 29, 2022), and with RoseTTAFold software (Baek et al., 2021) following the instructions of the website <https://robetta.bakerlab.org> (accessed September 26, 2022). Of the five models proposed by each program, those with the best prediction parameters were chosen. The study representations and graphs of protein structures were constructed with the help of the Discovery Studio Visualizer suite (v21.1.0) (<https://www.3dsbiovia.com/>; accessed April 26, 2022).

#### 4.16 | Molecular docking

The structure of adenosine monophosphate (AMP; PubChem CID 6083) is available in the PubChem database (<https://pubchem.ncbi.nlm.nih.gov/> [accessed June 10, 2022]). Docking was carried out with the structures obtained with AlphaFold2 and RoseTTAFold using Autodock 4.2 (<http://autodock.scripps.edu/> [accessed October 15, 2021]; Morris et al., 2009), as described elsewhere (Maiello et al., 2021). Initially, AMP docking was performed on a grid of  $126 \times 126 \times 126$  points, with a spacing of 0.375 angstroms, leading to a grid of  $47.25 \times 47.25 \times 47.25$  angstroms, which contained the entire structure of the protein. The grid was centered on the centroid of the protein. Fifty docking runs were performed, and the poses that were in the most populated cluster and with the lowest estimated free energy of binding were chosen to make a smaller grid. The process was repeated twice, and the last grid had  $126 \times 126 \times 126$  points, with a spacing of 0.125 angstroms, and with the center located in the centroid of the solution with the lowest estimated free energy of binding. One hundred docking runs were performed, and the best ranked pose was chosen (estimated free energy of binding =  $-7.04$  kcal/mol).

#### 4.17 | Sequence alignment and phylogenetic analysis

All the amino acid sequences used in this study are available in the National Center for Biotechnology Information (NCBI) sequence database (<https://www.ncbi.nlm.nih.gov/protein/>). Sequence alignment was performed using the ClustalW tool included in the Mega 11 suite (version 11.0.13; <http://www.megasoftware.net> [accessed October 8, 2022]; Tamura et al., 2021). Multiple sequence alignment was graphically represented by a sequence logo created with WebLogo 3 (<http://weblogo.threplusone.com/> [accessed October 8, 2022]). The evolutionary analysis was inferred by using the Maximum

Likelihood method as described elsewhere (Di Maro et al., 2014) and was conducted in MEGA 11 (Tamura et al., 2021). Representative sequences of uracil DNA N-glycosylases from bacteria were used as outgroup. The name and classification of fungi have been obtained from the Index Fungorum (<http://www.indexfungorum.org/>).

#### AUTHOR CONTRIBUTIONS

**Lucía Citores:** Formal analysis (equal); investigation (lead); methodology (equal); resources (equal); writing – review and editing (equal). **Sara Ragucci:** Formal analysis (equal); investigation (lead); methodology (equal); writing – review and editing (equal). **Rosita Russo:** Formal analysis (equal); investigation (equal); methodology (equal); writing – review and editing (equal). **Claudia C. Gay:** Investigation (equal); methodology (equal); writing – review and editing (supporting). **Angela Chambery:** Investigation (equal); methodology (equal); resources (equal); supervision (equal); writing – review and editing (equal). **Antimo Di Maro:** Formal analysis (equal); methodology (equal); resources (equal); writing – review and editing (equal). **Rosario Iglesias:** Conceptualization (equal); investigation (equal); methodology (equal); supervision (equal); writing – review and editing (equal). **José Miguel Ferreras:** Conceptualization (equal); investigation (equal); methodology (equal); resources (lead); supervision (equal); writing – original draft (lead); writing – review and editing (equal).

#### ACKNOWLEDGMENTS

This work was funded by grants BIO39/VA39/14 and BIO/VA17/15 (Consejería de Sanidad, Junta de Castilla y León) to Lucía Citores; grant VA033G19 (Consejería de Educación, Junta de Castilla y León) to the GIR ProtIBio; and MISE, project NUTRABEST PON I&C 2014–2020 Prog. n. F/200050/01-03/X45. Claudia C. Gay was supported by a fellowship from Programa de Movilidad entre todas las Instituciones Asociadas a la AUIP 2021—Segundo Plazo (Asociación Universitaria Iberoamericana de Postgrado).



#### CONFLICT OF INTEREST STATEMENT

The authors declare no conflict of interest.

#### DATA AVAILABILITY STATEMENT

The data that support the findings of this study are available from the corresponding author upon reasonable request.

#### ORCID

Antimo Di Maro  <https://orcid.org/0000-0002-9595-9665>  
 José M. Ferreras  <https://orcid.org/0000-0003-4816-5878>

## REFERENCES

- Afrin S, Rakib MA, Kim BH, Kim JO, Ha YL. Eritadenine from edible mushrooms inhibits activity of angiotensin converting enzyme in vitro. *J Agric Food Chem*. 2016;64:2263–8.
- Baek M, DiMaio F, Anishchenko I, Dauparas J, Ovchinnikov S, Lee GR, et al. Accurate prediction of protein structures and interactions using a three-track neural network. *Science*. 2021; 373:871–6.
- Barbieri L, Battelli MG, Stirpe F. Ribosome-inactivating proteins from plants. *Biochim Biophys Acta*. 1993;1154:237–82.
- Barbieri L, Stoppa C, Bolognesi A. Large scale chromatographic purification of ribosome-inactivating proteins. *J Chromatogr A*. 1987;408:235–43.
- Barbieri L, Valbonesi P, Bonora E, Gorini P, Bolognesi A, Stirpe F. Polynucleotide:adenosine glycosidase activity of ribosome-inactivating proteins: effect on DNA, RNA and poly(A). *Nucleic Acids Res*. 1997;25:518–22.
- Chung IM, Kim YJ, Moon HS, Han JG, Kong WS, Yarnes CT, et al. Improved accuracy of geographical origin identification of shiitake grown in sawdust medium: a compound-specific isotope model-based pilot study. *Food Chem*. 2022;369:130955.
- Citores L, Iglesias R, Ferreras JM. Ribosome inactivating proteins from plants: biological properties and their use in experimental therapy. In: Fang EF, Ng TB, editors. *Antitumor potential and other emerging medicinal properties of natural compounds*. Netherlands, Dordrecht: Springer; 2013. p. 127–43.
- Citores L, Iglesias R, Ferreras JM. Antiviral activity of ribosome-inactivating proteins. *Toxins (Basel)*. 2021;13:80.
- Citores L, Iglesias R, Ragucci S, Di Maro A, Ferreras JM. Antifungal activity of  $\alpha$ -Sarcin against *penicillium digitatum*: proposal of a new role for fungal ribotoxins. *ACS Chem Biol*. 2018;13: 1978–82.
- Citores L, Ragucci S, Ferreras JM, Di Maro A, Iglesias R. Ageritin, a ribotoxin from poplar mushroom (*Agrocybe aegerita*) with defensive and antiproliferative activities. *ACS Chem Biol*. 2019; 14:1319–27.
- Delforge D, Devreese B, Dieu M, Delaive E, Van Beeumen J, Remacle J. Identification of lysine 74 in the pyruvate binding site of alanine dehydrogenase from *Bacillus subtilis*. Chemical modification with 2,4,6-trinitrobenzenesulfonic acid, n-succinimidyl 3-(2-pyridyldithio)propionate, and 5'-(p-[fluoro-sulfonyl]benzoyl)adenosine. *J Biol Chem*. 1997;272:2276–84.
- Di Maro A, Citores L, Russo R, Iglesias R, Ferreras JM. Sequence comparison and phylogenetic analysis by the maximum likelihood method of ribosome-inactivating proteins from angiosperms. *Plant Mol Biol*. 2014;85:575–88.
- Di Maro A, Valbonesi P, Bolognesi A, Stirpe F, De Luca P, Siniscalco Gigliano G, et al. Isolation and characterization of four type-1 ribosome-inactivating proteins, with polynucleotide:adenosine glycosidase activity, from leaves of *Phytolacca dioica* L. *Planta*. 1999;208:125–31.
- Drohat AC, Maiti A. Mechanisms for enzymatic cleavage of the N-glycosidic bond in DNA. *Org Biomol Chem*. 2014;12:8367–78.
- Endo Y, Mitsui K, Motizuki M, Tsurugi K. The mechanism of action of ricin and related toxic lectins on eukaryotic ribosomes. The site and the characteristics of the modification in 28 S ribosomal RNA caused by the toxins. *J Biol Chem*. 1987; 262:5908–12.
- Endo Y, Wool IG. The site of action of alpha-sarcin on eukaryotic ribosomes. The sequence at the alpha-sarcin cleavage site in 28 S ribosomal ribonucleic acid. *J Biol Chem*. 1982;257: 9054–60.
- Fang EF, Ng TB. Ribonucleases of different origins with a wide spectrum of medicinal applications. *Biochim Biophys Acta*. 2011;1815:65–74.
- Girbés T, Ferreras J. Ribosome-inactivating proteins from plants. *Recent Res Dev Agric Biol Chem*. 1998;2:1–16.
- Grela P, Szajwaj M, Horbawicz-Drożdżal P, Tchorzewski M. How ricin damages the ribosome. *Toxins (Basel)*. 2019;11:241.
- Guo Q, Zhou W, Too HM, Li J, Liu Y, Bartlam M, et al. Substrate binding and catalysis in trichosanthin occur in different sites as revealed by the complex structures of several E85 mutants. *Protein Eng*. 2003;16:391–6.
- Hacker SM, Backus KM, Lazear MR, Forli S, Correia BE, Cravatt BF. Global profiling of lysine reactivity and ligandability in the human proteome. *Nat Chem*. 2017;9:1181–90.
- Hitomi K, Iwai S, Tainer JA. The intricate structural chemistry of base excision repair machinery: implications for DNA damage recognition, removal, and repair. *DNA Repair (Amst)*. 2007;6: 410–28.
- Iglesias R, Citores L, Di Maro A, Ferreras JM. Biological activities of the antiviral protein BE27 from sugar beet (*Beta vulgaris* L.). *Planta*. 2015;241:421–33.
- Iglesias R, Citores L, Ferreras JM. Ribosomal RNA N-glycosylase activity assay of ribosome-inactivating proteins. *Bio Protoc*. 2017;7:e2180.
- Iglesias R, Citores L, Ragucci S, Russo R, Di Maro A, Ferreras JM. Biological and antipathogenic activities of ribosome-inactivating proteins from *Phytolacca dioica* L. *Biochim Biophys Acta*. 2016;1860:1256–64.
- Iglesias R, Russo R, Landi N, Valletta M, Chambery A, Di Maro A, et al. Structure and biological properties of ribosome-inactivating proteins and lectins from elder (*Sambucus nigra* L.) leaves. *Toxins (Basel)*. 2022;14:611.
- Jumper J, Evans R, Pritzel A, Green T, Figurnov M, Ronneberger O, et al. Highly accurate protein structure prediction with AlphaFold. *Nature*. 2021;596:583–9.
- Kobayashi H, Hara J, Itagaki T, Inokuchi N, Koyama T, Sanda A, et al. Relationship of two ribonucleases with molecular masses of 45 kDa and 37 kDa from the culture medium of *Lentinus edodes*. *Biol Pharm Bull*. 2000;23:800–4.
- Kobayashi H, Kumagai F, Itagaki T, Inokuchi N, Koyama T, Iwama M, et al. Amino acid sequence of a nuclease (nuclease Le1) from *Lentinus edodes*. *Biosci Biotechnol Biochem*. 2000; 64:948–57.
- Lam SK, Ng TB. First simultaneous isolation of a ribosome inactivating protein and an antifungal protein from a mushroom (*Lyophyllum shimeji*) together with evidence for synergism of their antifungal effects. *Arch Biochem Biophys*. 2001;393: 271–80.
- Landi N, Hussain HZF, Pedone PV, Ragucci S, Di Maro A. Ribotoxic proteins, known as inhibitors of protein synthesis, from mushrooms and other fungi according to Endo's fragment detection. *Toxins (Basel)*. 2022;14:403.
- Landi N, Ragucci S, Citores L, Clemente A, Hussain HZF, Iglesias R, et al. Isolation, characterization and biological action of Type-1 ribosome-inactivating proteins from tissues of *Salsola soda* L. *Toxins (Basel)*. 2022;14:566.
- Landi N, Ragucci S, Russo R, Pedone PV, Chambery A, Di Maro A. Structural insights into nucleotide and protein sequence of



- Ageritin: a novel prototype of fungal ribotoxin. *J Biochem.* 2019;165:415–22.
- Lu JQ, Shi WW, Xiao MJ, Tang YS, Zheng YT, Shaw PC. Lyophilin, a mushroom protein from the peptidase M35 superfamily is an RNA N-glycosidase. *Int J Mol Sci.* 2021;22:11598.
- Maiello S, Iglesias R, Polito L, Citores L, Bortolotti M, Ferreras JM, et al. Sequence, structure, and binding site analysis of Kirkiin in comparison with ricin and other type 2 RIPs. *Toxins (Basel).* 2021;13:862.
- Monteuuis G, Wong JLL, Bailey CG, Schmitz U, Rasko JEJ. The changing paradigm of intron retention: regulation, ramifications and recipes. *Nucleic Acids Res.* 2019;47:11497–513.
- Morris GM, Huey R, Lindstrom W, Sanner MF, Belew RK, Goodsell DS, et al. AutoDock4 and AutoDockTools4: automated docking with selective receptor flexibility. *J Comput Chem.* 2009;30:2785–91.
- Ngai PH, Ng TB. Lentin, a novel and potent antifungal protein from shiitake mushroom with inhibitory effects on activity of human immunodeficiency virus-1 reverse transcriptase and proliferation of leukemia cells. *Life Sci.* 2003;73:3363–74.
- Nguyen AH, Gonzaga MI, Lim VM, Adler MJ, Mitkov MV, Cappel MA. Clinical features of shiitake dermatitis: a systematic review. *Int J Dermatol.* 2017;56:610–6.
- Niego AG, Rapior S, Thongklang N, Raspe O, Jaidee W, Lumyong S, et al. Macrofungi as a nutraceutical source: promising bioactive compounds and market value. *J Fungi (Basel).* 2021;7:397.
- Olombrada M, Lazaro-Gorines R, Lopez-Rodriguez JC, Martinez-Del-Pozo A, Onaderra M, Maestro-Lopez M, et al. Fungal ribotoxins: a review of potential biotechnological applications. *Toxins (Basel).* 2017;9:71.
- Ragucci S, Bulgari D, Landi N, Russo R, Clemente A, Valletta M, et al. The structural characterization and antipathogenic activities of Quinoin, a type 1 ribosome-inactivating protein from quinoa seeds. *Int J Mol Sci.* 2021;22:8964.
- Ragucci S, Russo R, Landi N, Valletta M, Chambery A, Esposito S, et al. Muskox myoglobin: purification, characterization and kinetics studies compared with cattle and water buffalo myoglobins. *J Sci Food Agric.* 2019;99:6278–86.
- Saxena SK, Rybak SM, Winkler G, Meade HM, McGray P, Youle RJ, et al. Comparison of RNases and toxins upon injection into xenopus oocytes. *J Biol Chem.* 1991;266:21208–14.
- Sharma VP, Kamal S, Singh M. Species and region-wise mushroom production in leading mushroom producing countries—China, Japan, USA, Canada and India. *Mushroom Res.* 2022;30:99–108.
- Sheng K, Wang C, Chen B, Kang M, Wang M, Liu K, et al. Recent advances in polysaccharides from *Lentinus edodes* (Berk.): isolation, structures and bioactivities. *Food Chem.* 2021;358:129883.
- Tamura K, Stecher G, Kumar S. MEGA11: molecular evolutionary genetics analysis version 11. *Mol Biol Evol.* 2021;38:3022–7.
- Zhu F, Zhou YK, Ji ZL, Chen XR. The plant ribosome-inactivating proteins play important roles in defense against pathogens and insect Pest attacks. *Front Plant Sci.* 2018;9:146.

## SUPPORTING INFORMATION

Additional supporting information can be found online in the Supporting Information section at the end of this article.

**How to cite this article:** Citores L, Ragucci S, Russo R, Gay CC, Chambery A, Di Maro A, et al. Structural and functional characterization of the cytotoxic protein ledodin, an atypical ribosome-inactivating protein from shiitake mushroom (*Lentinula edodes*). *Protein Science.* 2023;32(4):e4621. <https://doi.org/10.1002/pro.4621>